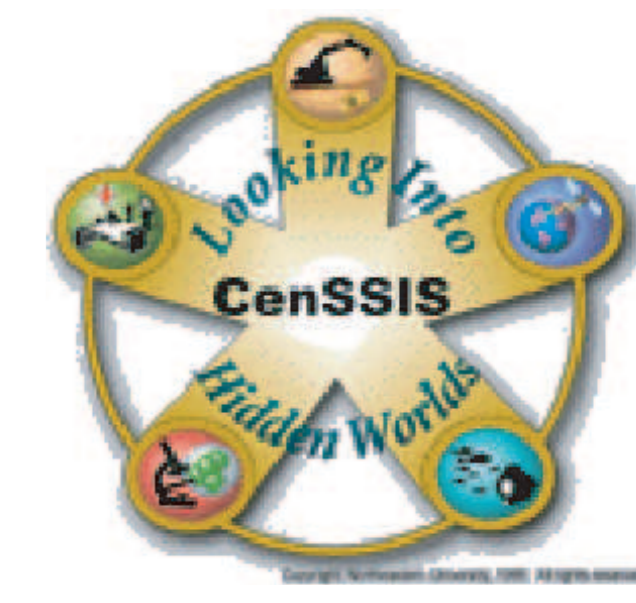




X-RAY TOMOSYNTHESIS ELASTOGRAPHY: A FEASIBILITY STUDY.

Michael S. Richards¹, Paul E. Barbone², Tao Wu³, Richard H. Moore³ and Daniel B. Kopans³
Boston University, Boston MA 02215.



Abstract

X-ray tomosynthesis is an imaging modality which reconstructs 3D tissue volumes from multiple planar X-ray images taken at different angles relative to the sample volume. Specifically, tomosynthesis mammography is used for imaging 3-D breast volumes to aid in the detection and diagnosis of breast cancers. Elastography is being considered as an additional tool to enhance this imaging modality. Due to the nature of the tomosynthesis mammography examination, the breast is under a controlled compression while being imaged. At least two 3-D images, under different compressions, need to be obtained during testing to obtain a strain image. A third image of the breast under shear will be required to reconstruct the tissue modulus. Images have high resolution in planes parallel to the X-ray detector and less resolution in the direction perpendicular to the detector.

Gelatin phantoms have been created with calcium particles intermixed to generate speckled images for displacement tracking. Phantoms were created with varying modulus distribution by controlling the concentration of gelatin. Initial images show that the phantoms closely match the attenuation of the breast tissue. Preliminary analysis of the displacement was done using a three dimensional cross correlation algorithm. Initial results show good tracking with resolutions in the millimeter range for the planes perpendicular to the imaging detector. A 3-D finite element code will be used to reconstruct the modulus images in future experiments. The purpose of this study is to determine if tomosynthesis mammography can be used to track tissue displacement and ultimately quantitatively measure the elastic properties of breast tissue.

X-Ray Tomosynthesis Elastography

We have begun an investigation into the feasibility of using three dimensional X-ray tomosynthesis to quantitatively image the mechanical properties of breast tissue. In this study we determined a protocol for creating tissue-mimicking phantoms for tomosynthesis elastography. Our group collaborates with Massachusetts General Hospital to develop an experimental protocol and image our phantoms. We have adapted an algorithm for displacement and strain estimation in three dimensions and consider what, in the future, will be needed to reconstruct elastic modulus images.

Background and Motivation

Tomosynthesis

- This imaging modality produces 3-D X-ray images of breast volumes. It requires several X-ray images, each taken with the X-ray source at a different position relative to the detector and the tissue being imaged. If the X-ray source position is changed, the path length of the X-rays is altered thus changing the interference of tissue in those path lengths. If the position of the source is known, a computer algorithm is used to reconstruct 3-D images of the tissue volumes from these individual images. The over all exposure level the tomosynthesis system requires for one image reconstruction is typically ~50% higher than that of a single film 2-D mammogram.
- Our collaborators clinically test this imaging modality for use in breast cancer detection (tomosynthesis mammography). The hope is that this imaging technique will reduce false-positive and false-negative diagnoses when compared to conventional 2-D mammography [5]. X-ray mammography is one of the leading tools for diagnosing breast cancer and is highly accessible to clinicians.

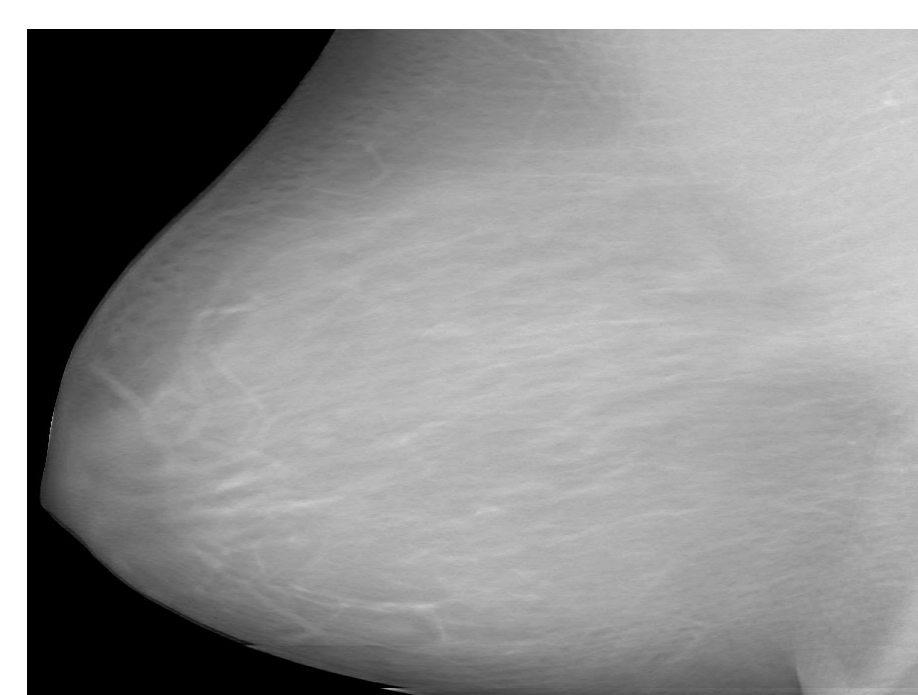


Figure 1. Typical Slice of Tomosynthesis Breast Image.

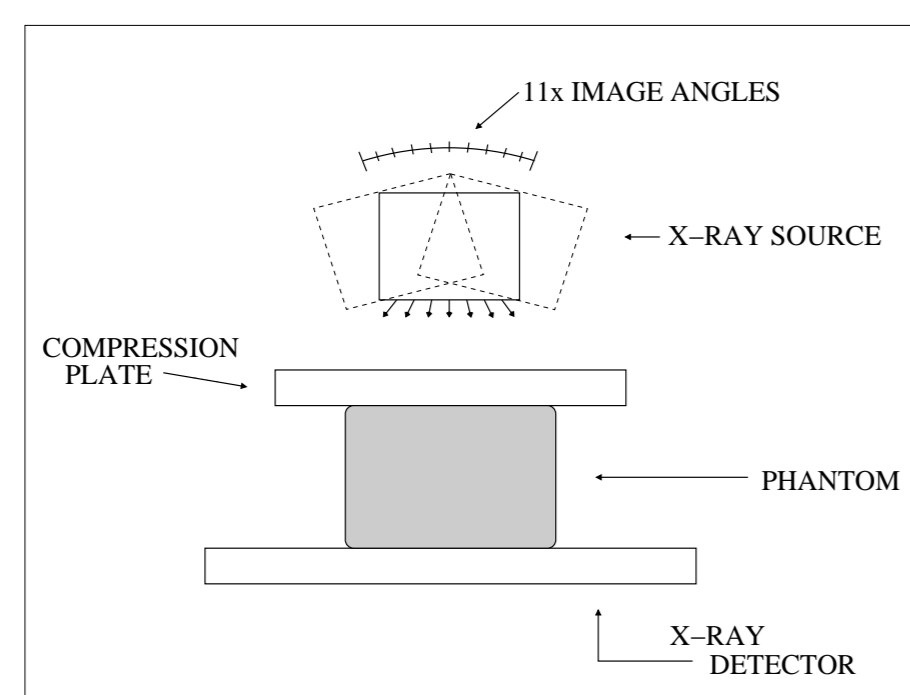


Figure 2. Imaging setup.

Elastography

- One characteristic of clinical mammography is that the breast is held in compression between the X-ray detector and a compression plate. This practice motivates the integration of elastography into this imaging modality. Elastography is a method of imaging tissue stiffness by comparing images taken of tissue while it is being mechanically perturbed. Tissue stiffness or elastic modulus distribution is believed to be clinically significant and may be correlated to tumor histology [4].

- One advantage of integrating elastography into this imaging modality is that it would create strain and elastic modulus images in perfect registration with the tomosynthesis mammograms, thus further improving the diagnostic accuracy of this system. It would also produce a reproducible 3-D image of a quantity that physicians routinely probe by manual palpation.
- The motivation behind quantitatively reconstructing the elastic modulus is to uniquely identify specific regions of the breast which are stiffer than normal tissue. Quantitative segmentation of modulus values can increase diagnostic accuracy and repeatability for multiple patient visits or consistency between patients.

Experimental And Analytical Methods

Phantom Construction

- Elastic tissue mimicking phantoms were created using a gelatin base. Inclusions, made to mimic tumor stiffness, were added to the phantoms by altering gelatin concentration in discrete areas of the phantom. Chalk particles (CaCO_3) were used to introduce features to the phantom, mimicking attenuation differences found between blood vessels, calcium deposits and the surrounding tissue. Calcium Carbonate was used because it is strong absorber of X-rays. Chalk concentration was made to approximate attenuation in breast tissue, 2.0% by mass [2],[3]. Gelatin, with a bloom strength of 300, was concentrated at 10.0% or 15.0% by mass, depending on the relative stiffness required. The cuboidal inclusions were made with 15% gelatin and the background was 10%. Prior to letting any phantom material set, all ingredients were degassed as a mixture.



Figure 3(a) and (b). Tissue Phantoms with Inclusions.

Imaging Protocol

- Images of the phantom were taken at 11 projection angles over a 50° range [5]. During imaging, the phantoms were placed between the compression plate and the detector with a precompression of several millimeters. Paper was placed between the detector and the phantom which approximately enforced zero displacement boundary conditions.
- Image sets (11 images per reconstructed image volume) were taken for incrementally increasing compression. Image reconstructions are found using an iterative Maximum Likelihood algorithm described in [5]. The original images and the reconstructions have high resolution in directions parallel to the plane of the image detector (~0.1 mm/voxel) and poor resolution in the direction perpendicular to it (~1.0 mm/voxel).

Displacement and Strain Estimation

- Displacements between reconstructions were estimated using 3-D cross-correlation algorithm adapted from a 2-D Particle Image Velocimetry algorithm, "URAPIV" [1]. Small, equally sized 3-D blocks were taken from the same position in each reconstructed image and the peaks of their cross correlations were taken to be the displacements. The size of the blocks and the overlap of each are user defined in all directions and can be optimized to the data set. Correlations were done using a 3-D Fourier transform and the peaks of the data were interpolated with a Gaussian to approximate sub-pixel displacements. The process was done for many equally spaced blocks which span the entire volume, creating an estimated 3-D vector field of displacements.
- Strain estimates were evaluated two dimensionally in planes parallel to the imaging detector (high resolution directions). Local strains were calculated by a least squares fit to small displacement planes cut from a whole plane. The smaller planes are equally spaced and span the entire plane. Size of the smaller planes and amount of overlap between planes is also user defined.

Results

- Phantom image volumes were reconstructed, creating ~40 image slices similar to that shown in Figure 4. One reconstructed volume was found for each of four different applied displacement experiments. The initial height was 40 mm and the other images were taken at heights of 39, 38, and 35 mm. This allows us to calculate displacements for differences of 1.0 mm through 5.0 mm. Currently, only millimeter displacement increments are allowed by nature of the compression plate.
- Displacements were found for all directions. Individual block dimensions were approximately 4 mm x 4 mm x 8 mm in the X, Y (high resolution) and Z (low resolution) directions, respectively. The overlap of each block was half the block dimensions in each direction. Displacements were calculated separately for all applied displacement variations.
- Strain estimates were found separately for each imaging plane in the X and Y directions using the least squares fit of the incremental plane sizes which were 15 x 15 displacement vectors in each direction. Strains which required displacements in the low resolution direction were not calculated.

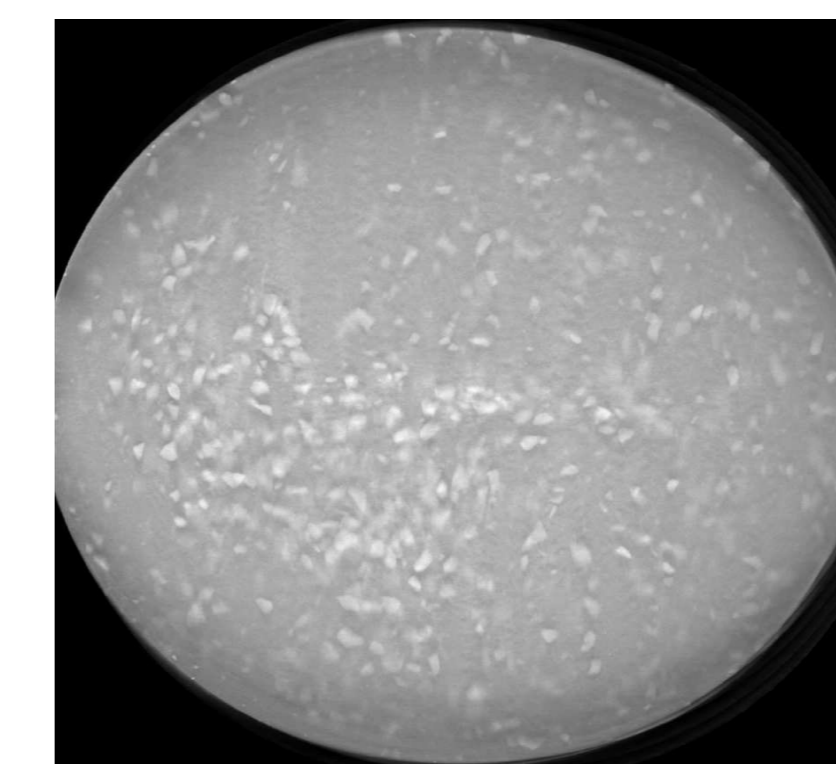


Figure 4. Typical Slice of Reconstructed Phantom Image.

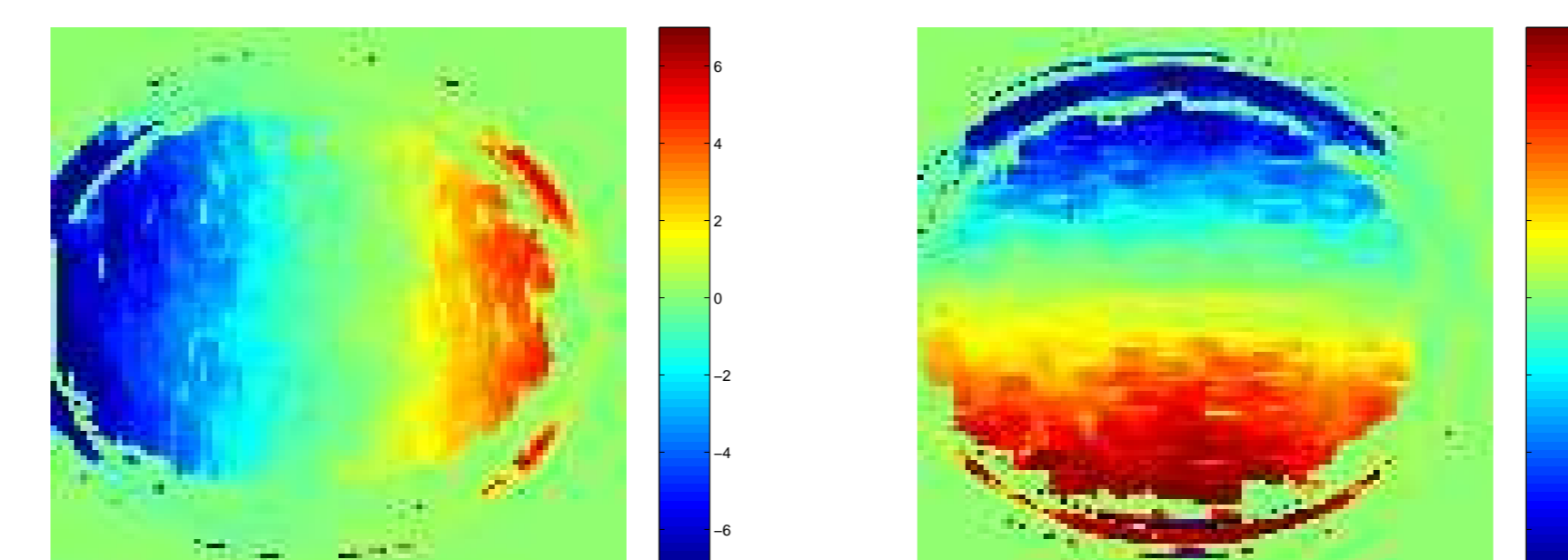


Figure 5(a) and (b). Typical Displacement Images for the X and Y Directions for One Plane (u and v , Respectively).

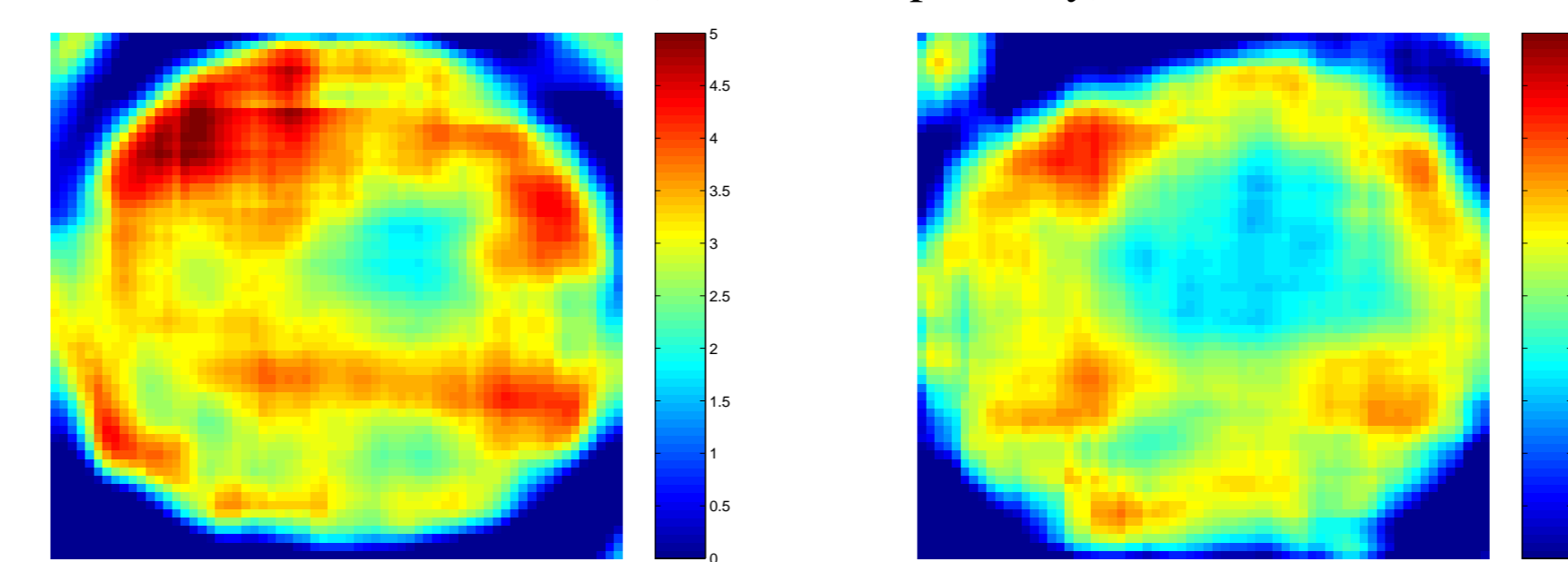


Figure 6(a) and (b). Typical Strain Images for Two Different Planes ("Strain" = $\partial u/\partial x + \partial v/\partial y$).

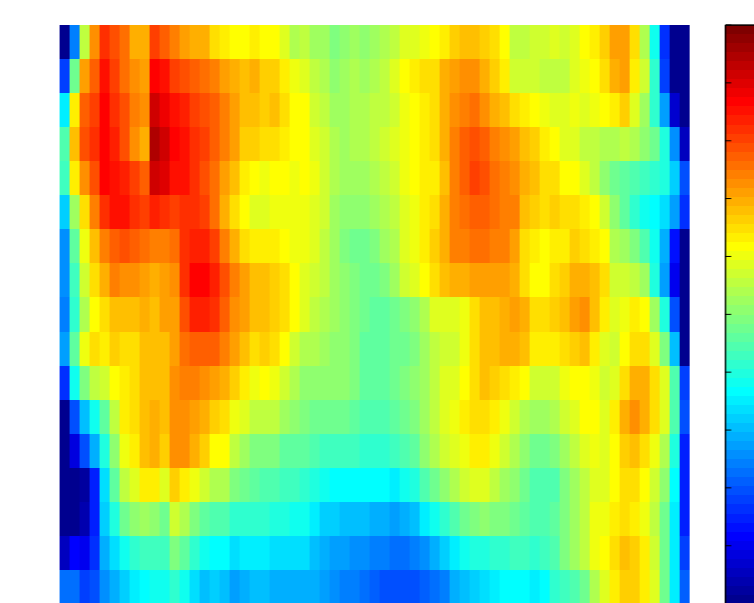


Figure 7. Typical Strain Image in the X-Z Plane ("Strain" = $\partial u/\partial x + \partial v/\partial y$).

Discussion

- Image reconstructions of the phantoms distinguished the backgrounds from larger chalk particles with high accuracy. Smaller chalk particles seemed only to add to the background attenuation. The background has no distinguishable features and signal to noise ratio are relatively low.
- Calculated displacement images seemed consistent with experimental methods. There is a high level of displacement on the outer borders of the cylinder and zero measured displacement close to the center of the phantom. The measured displacement in the direction of low resolution was highly noisy, however, overall it seemed to match up with experimentally applied displacements.
- Calculated strain images were harder to interpret for several reasons. First, the abnormal size and geometry of the inclusions made it unclear what the

expected strain image should look like. Also, the zero strain boundary condition on the bottom may have added large artifacts to our strain image. Strain images of simulated phantom data can be seen in Figure 8. Both images are constrained on the bottom boundary and compressed as our phantoms were. Strain artifacts are present in both images and are slightly more prominent in the image with inclusions. Lastly, the signal to noise ratio in the displacements are large which caused problems for differentiation. The low signal to noise ratios were seen in areas with low concentration of chalk particles.

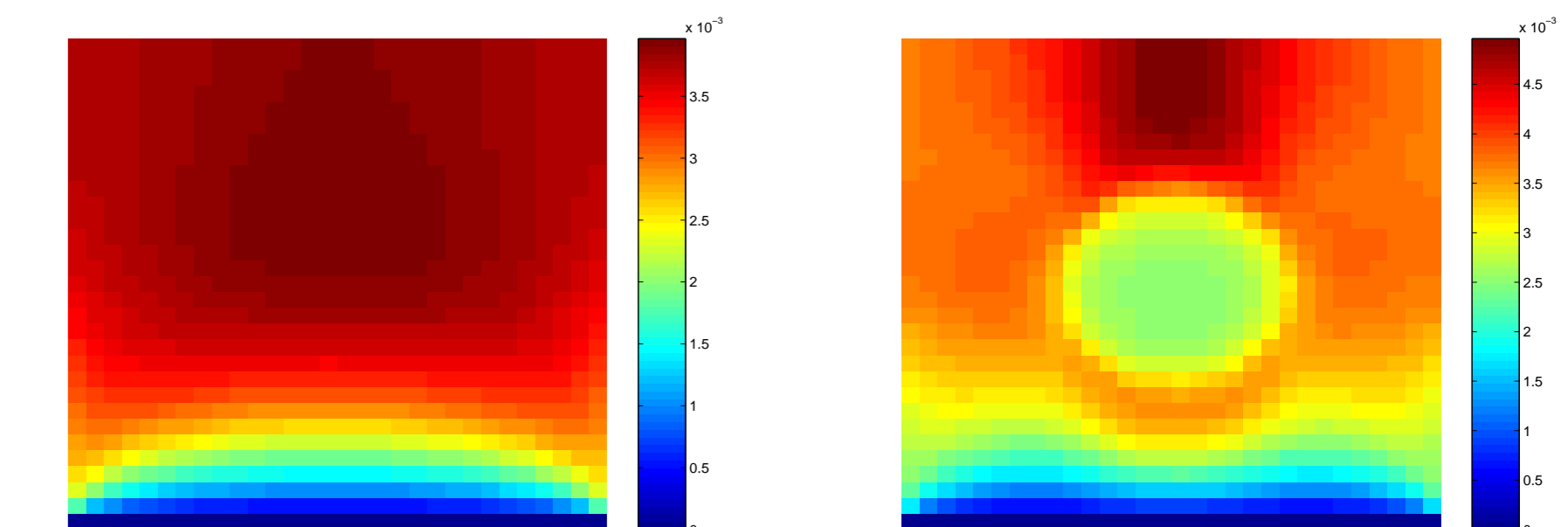


Figure 8(a) and (b). Strain Image in the X-Z Plane of Simulated Phantom Material With (a) and Without (b) an Inclusion ("Strain" = $\partial u/\partial x + \partial v/\partial y$).

Future Work

- Redesigned phantoms are being made with inclusions which will have predictable strain fields and the boundary conditions of the experiment during imaging will be controlled to allow for better interpretation of strain images. Phantoms are also being altered to increase the concentration of the larger chalk particles with the hope that the feature density will increase thus decreasing the signal to noise ratio.
- A further motivation of this study is to use displacement and strain fields to determine, quantitatively, the tissue modulus field. To do this, however, more information needs to be collected to solve the inverse partial differential equation (PDE). For instance, a second set of images with a different imposed mechanical perturbation (shear strain) must be obtained to solve the PDE using a direct method. The set up of the tomosynthesis system is such that imposing a shearing motion with the compression plate is a simple modification.

Acknowledgments

This work was supported in part by CenSSIS (The Center for Subsurface Sensing and Imaging) under the Engineering Research Centers Program of the National Science Foundation (Award No. EEC-9986821).

References

- [1] Roi Gurka and Alex Liberzon. Computation of pressure distribution using piv velocity data. In *3rd International Workshop on Particle Image Velocimetry*, September 1999.
- [2] P Homolka, A Gahleitner, M Prokop, and R Nowotny. Optimization of the composition of phantom materials for computed tomography. *Physics in Medicine and Biology*, 47:2907–2916, 2002.
- [3] M E Polletti, O D Goncalves, and I Mazzaro. X-ray scattering from human breast tissues and breast-equivalent materials. *Physics in Medicine and Biology*, 47:47–63, 2002.
- [4] P.Wellman, R.H.Howe, E. Dalton, and K.A.Kern. Breast tissue stiffness in compression is correlated to histological diagnosis. Technical report, Harvard Birobotics Laboratory, 1999.
- [5] T Wu, R Moore, D Kopans, A Stewart, W Phillips, M Stanton, J Eberhard, B Opsahl-Ong, L Niklason, and M Williams. Tomosynthesis mammography reconstruction using a maximum likelihood method. *Medical Physics*, 30(6):1332, 2003.

¹ Department of Biomedical Engineering, Boston University, Boston MA.

² Department of Aerospace and Mechanical Engineering, Boston University, Boston MA.

³ Massachusetts General Hospital, Boston MA.